

## A MODEL STUDY OF ROCK-JOINT DEFORMATION

N. R. BARTON

Norwegian Geotechnical Institute, Oslo, Norway

(Received 13 November 1971)

**Abstract**—Existing techniques of rock-joint modelling are reviewed. It is concluded that no methods presently in use are acceptable as either realistic models of mating rock joints or as mass production methods for the development of large, highly jointed models of rock masses.

A method is described for producing mating tension fractures in a weak, brittle model material using a large guillotine device. Parallel sets of model joints can be produced which are continuous, cross-jointed or offset (stepped) depending upon the chronological order of fracturing. The direct shear properties of these three types are compared and evaluated. The model results are used as a basis for predicting the full-scale (1:500) displacements accompanying shear failure of a 96-ft long prototype tension joint.

Recent numerical modelling of jointed rock masses has been based on assumed values of the shear and normal stiffness of the joints. These components are found to dominate the elastic deformation properties of the intact rock. The results of shear and normal stiffness tests on the model joints are used for a careful assessment of these quantities. The shear stiffness (peak shear stress per unit tangential displacement) is found to be both normal stress and size dependent, and this is confirmed by a survey of shear-test data for joints in rock. There appears to be an inverse proportionality between test dimension and shear stiffness, for a given normal stress. The normal stiffness (normal stress per unit closure) is found to be dependent on the preconsolidation or virgin normal stress level.

The problems of simulating the behaviour of jointed rock masses by the finite-element method are reviewed. Two particular drawbacks seem to be the conservation of energy demanded during computation, and the computer storage problems involved in modelling dilatant joints. Both these features are of fundamental importance to rock-mass deformation. A move towards realistic physical modelling is considered essential to an understanding of real processes.

### INTRODUCTION

IT IS COMMONLY believed that stress concentrations exist around the toe of steep rock slopes. This belief is the result of numerical elastic stress distributions, in which the assumption is made that the joints that exist do not deform, and therefore do not alter the elastic stress system. Recent numerical and physical model studies have thrown considerable doubt on the relevance of such assumptions. In fact, for numerical or physical model analyses to be realistic, attention has to be paid to the strength and deformation properties of the joints, almost to the exclusion of the intact rock between the joints.

This difficult problem has now been partially solved using more sophisticated finite element and difference techniques (GOODMAN *et al.* [1], MAHTAB and GOODMAN [2], ZIENKIEWICZ *et al.* [3], ST JOHN [4] and CUNDALL [5]). However, the fundamental problem of realistic input data has not been adequately tackled and the numerical analyses fall short of reality as a result.

Unfortunately, *in situ* shear tests and plate-jacking tests are extremely expensive and time consuming. In addition their relevance is in question since it is not certain what test dimensions are most relevant to a given problem. It is believed that useful guidelines can be

supplied by realistic physical models, and at only a fraction of the cost. A limited and more specific *in situ* programme can be planned as a result. This paper was written with this aim in mind.

The shear characteristics of interlocking rock surfaces are dependent to a large extent on several phenomena of intact rock failure. It would seem therefore that a realistic model material must first scale the properties of intact rock. If geometrically scaled joint surfaces can then be produced in the model material, there is a good chance of correct scaling of the discontinuous properties which, taken separately, are far more important in rock engineering than the intact properties, but in reality are inseparably linked to them. Two features of particular importance have to be considered, when producing artificial model joints.

Firstly, direct shear characteristics for the joints showing an 'unstable' mode of failure rather than a 'stable' mode have to be created by some means. That is to say, a graph of shear strength vs shear displacement is required which shows a marked drop from a peak strength at small displacements to a lower residual strength at large displacements. This would be in direct contrast to one showing stable characteristics in which the maximum strength is reached followed by unchanging shear resistance with increasing shear displacement. The contrasted effects of these two modes on the progressive failure of a rock slope is an obvious illustration of their importance.

Secondly, when an unstable mode of failure has been successfully simulated, the technique involved must be critically examined for its practical possibilities. A recent study of rock-slope behaviour was performed using a large 'two-dimensional' jointed model (BARTON [6]). Before each model was constructed four days were spent in generating joint sets through intact 1-in. thick slabs of the model material. Approximately forty thousand discrete blocks were produced in this short period and this of course implies that some mass-production technique was employed. In addition, the joints could be generated in parallel sets in any desired direction, so as to intersect previous sets at any angle.

#### *Previous methods of joint simulation*

A most comprehensive review of rock mechanics modelling was published by STIMPSON [7]. It is apparent that joint modelling has received a minimum of attention in the past. Of the limited number of techniques in use, many are suspect from several points of view.

The simplest technique which is widely used is to cast discrete blocks of model material in smooth-sided moulds. When these are cured the prototype structure is simulated by packing the blocks into a model loading frame, usually in the form of a 'two-dimensional' wall. A regular packing is most frequently employed, such that two orthogonal 'joint sets' are produced.

The next logical step is to find some means of varying (increasing) the frictional properties of the smooth-mating block faces. Several authors have reported the variable angle of friction that can be achieved by inserting various materials between the flat faces of cast bricks or layers of the model material. FUMAGALLI [8] has achieved friction angles as high as 40–46° by inserting sand of various grain sizes. However, it would appear that this might tend to produce a markedly stable joint behaviour rather similar to the residual of rock joints. This residual strength is largely controlled by sliding and rolling in the intermittent bed of debris which builds up between shearing surfaces after large displacements.

LADANYI and ARCHAMBAULT [9] and KRSMANOVIC *et al.* [10] tackled the problem of joint roughness rather more directly. Imbricated (stepped) surfaces were produced by interlocking the model bricks. These could be set at various angles and with various heights of

step. Total 'friction angles' of between 40 and 60° were obtained by the second authors. These angles were dependent on both the height of the steps and the normal stresses. However, it seems likely that this form of joint would tend to produce some cohesion intercept when the direction of shearing was against the steep sides of the blocks. No details were given of this directional dependence.

PATTON [11] produced interlocking teeth joints by casting directly against moulds with teeth. These teeth, ranging from 15 to 45° inclination and with 90° ends, produced his well-known bilinear approximation to peak shear-strength envelopes, and obvious drops from peak to residual strength. None of the above methods seem to be practical possibilities where large, highly jointed models are required.

#### *Tension fracture method of joint simulation*

The method to be described in this paper was accidentally conceived. It was found that a new, weak brittle model material could be split into rough fractures extremely easily, when cast blocks were gently tapped with a chisel. The realistic intact properties of this model material were chiefly to blame for this discovery, and they will be very briefly described. (A detailed report of the mechanical properties of the material has been published elsewhere —BARTON [12]).

The material is formed from an oven-cured combination of red lead-sand/ballotini-plaster-water. Unconfined compression strengths ( $\sigma_c$ ) as low as 5 lbf/in<sup>2</sup> can be obtained, and the Brazilian tensile strengths ( $\sigma_t$ ) range from one-seventh to one-tenth of the compression strengths. The axial load-deformation curves are typically flat 'S' shaped, with failure occurring in a brittle manner at an axial strain ( $\epsilon\%$ ) which can be varied from approximately 0.25 to 0.45 per cent. The modulus ratio ( $E/\sigma_c$ ) can also be varied at will, within the range 350–560. The Mohr rupture envelopes for a range of confining pressure from 0 to 3.5 lbf/in<sup>2</sup> were typically curved in shape, and the shear strength could also be varied by using different ratios of sand/ballotini. A ratio of 100:0 produced a markedly steeper Mohr envelope than a ratio of 0:100 of the frictional component. The high-density red-lead filler gave a curved density ( $\rho$ ) of between 120 and 125 lbf/ft<sup>3</sup>, roughly four fifths that of rock.

The particular compound used in the model study referred to earlier was termed C3. Choosing a geometric scale ( $\lambda$ ) of 1 to 500, the resulting stress scale ( $\psi$ ) for a gravitationally loaded model is approximately 1 to 666, assuming a prototype density of 160 lbf/ft<sup>3</sup>. The model-prototype mechanical properties can be summarized as follows:

TABLE 1. MODEL-PROTOTYPE PROPERTIES OF MATERIAL C3

Symbol	Model (C3)	Units	Prototype
$\sigma_c$	20.1	lbf/in <sup>2</sup>	13,400
$\sigma_t$	2.4	lbf/in <sup>2</sup>	1600
$E$	$1.07 \times 10^4$	lbf/in <sup>2</sup>	$7.13 \times 10^6$
$\epsilon$	0.31	%	0.31
$\rho$	121.2	lbf/ft <sup>3</sup>	160

The properties of most relevance to easy tensile splitting are the low tensile strength (2.4 lbf/in<sup>2</sup>) and the relative brittleness, which is reflected in the realistic axial strain at failure (0.31 per cent).

Initially a small guillotine was designed on classic French principles. This could generate tension fractures through small rectangular blocks of the model material, using the momentum of a single falling blade. The experience gained was used in the design of the large guillotine shown in Fig. 1. This has two opposed parallel blades which are driven to strike simultaneously the top and bottom surface of a 1-in. thick slab, placed on the slotted table. After each fracture the slab and slotted table are translated exactly  $\frac{1}{2}$  in. in a direction perpendicular to the common blade tracks. When the electrically driven blades are next operated, a second fracture is generated parallel to the first, and  $\frac{1}{2}$  in. away. This simple principle is illustrated in Fig. 2.

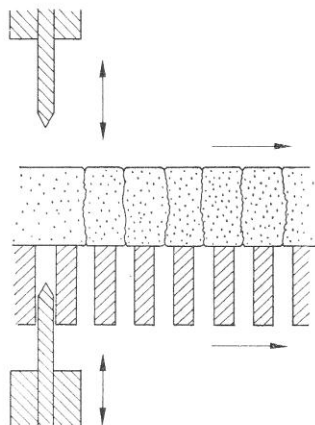


FIG. 2. Section showing the splitting mechanism and the typical non-linearity of the fractures.

Figure 3 shows six sequence photographs of a 16-in. square, 1-in. thick slab being split into one, two and finally three sets of parallel fractures. The slab is thereby split into approximately 2000 separate blocks. The whole operation takes only 1 hr.

#### *Model fracture genesis*

The tension fractures are generated as a result of slight extension caused by limited surface penetration of the opposed  $60^\circ$  blades. (This is carefully controlled.) The fractures are in fact slightly open after they are formed. Measurements have indicated that when orthogonal joint sets are developed parallel and perpendicular to the slab edges, an increase in the dimensions of approximately 1 per cent occurs. In other words a slab of dimensions 16 in.  $\times$  16 in.  $\times$  1 in. when cast, becomes 16.15 in.  $\times$  16.15 in.  $\times$  1 in. when jointed symmetrically in two directions, at  $\frac{1}{2}$  in. spacing. This means that 31 fractures have a total width of 0.15 in. and therefore each model joint is approximately 0.005 in. wide when in this (almost) unstressed state. As will be seen presently, these gaps close irrecoverably under normal stress, and the jointed model then deforms in direct response to its subsequent loading history.

A feature of great interest is that the first joint set (primary) to be developed through a slab is the only set which has continuous, unbroken fractures. Each subsequent set (secondary, tertiary, etc.) is offset where it crosses a pre-existing fracture. This is contrary to the

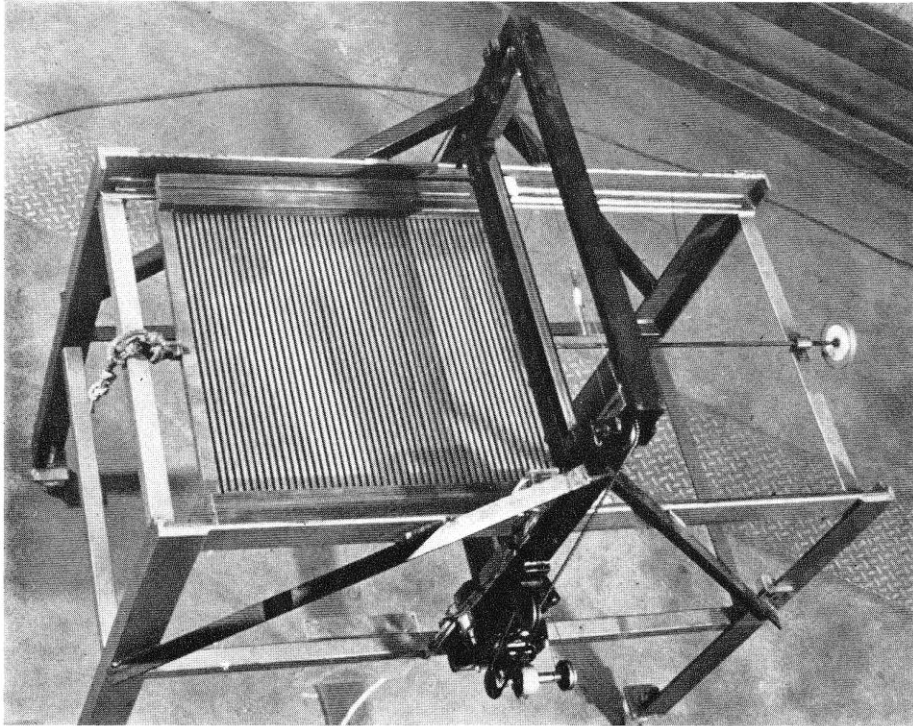


FIG. 1. The large guillotine used for generating model joint sets through slabs of the model material.

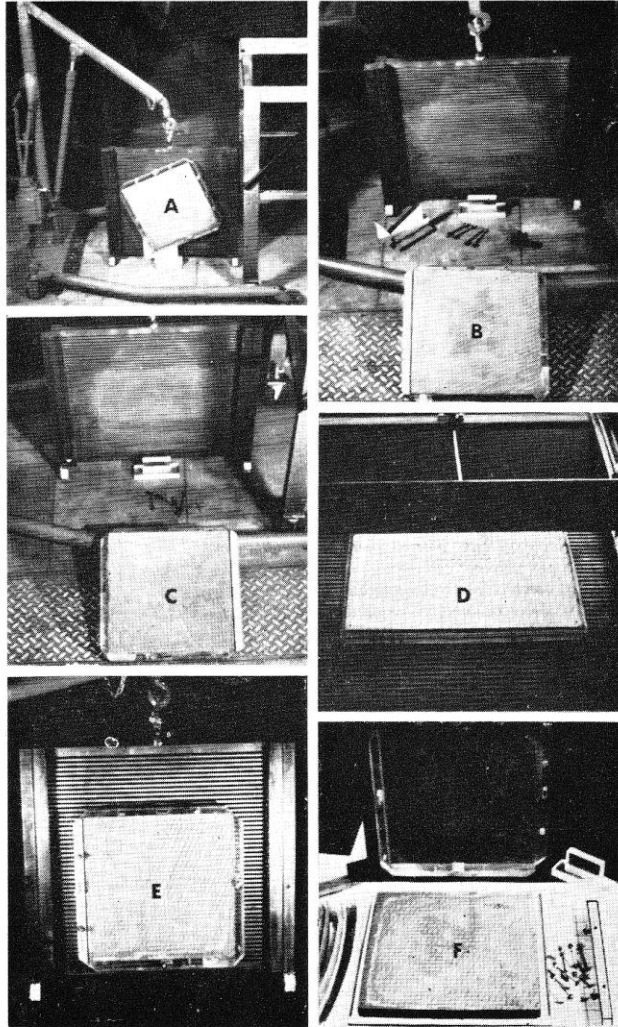


FIG. 3. Six sequences in the production of a jointed slab.

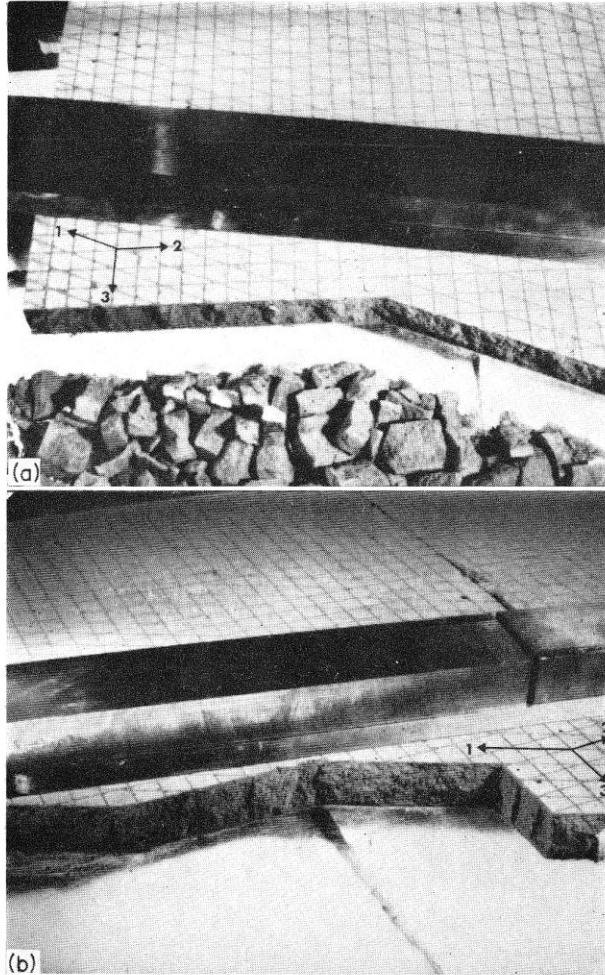


FIG. 4. The model joint surfaces produced by three intersecting joint sets.

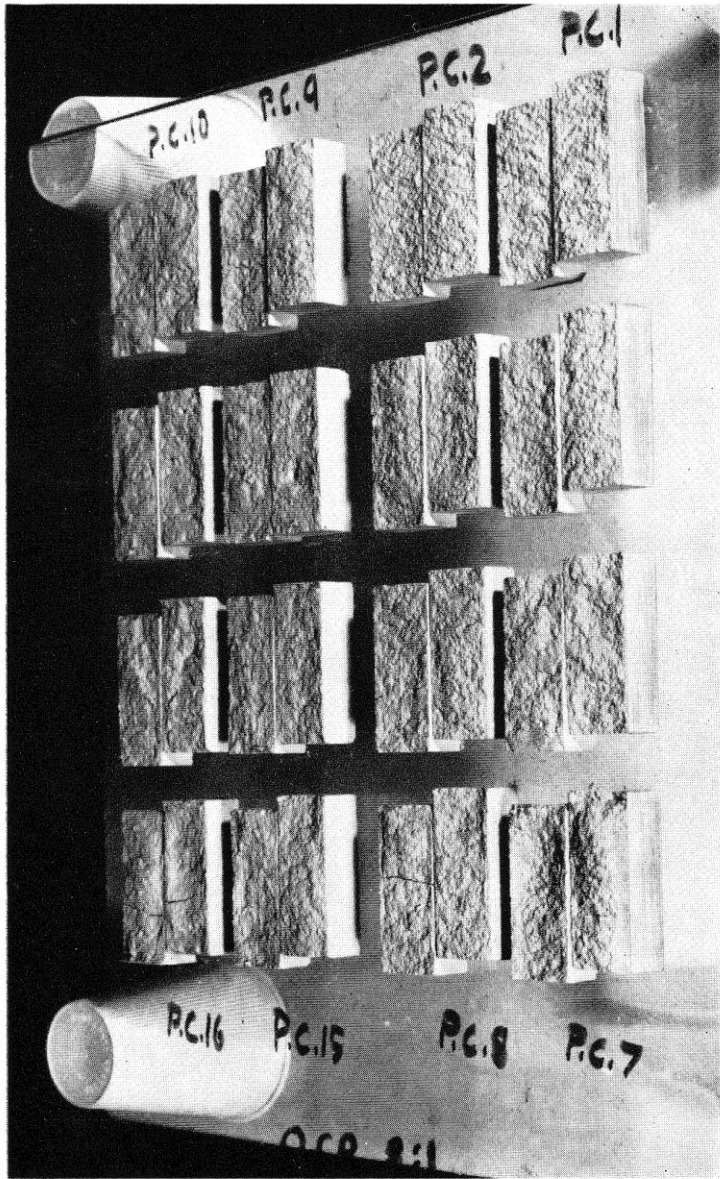


FIG. 6. The surface damage caused by shearing at different normal stresses.

impression created by the straight blade marks on the surface of the slabs. Figures 4 and 5 illustrate these internal features. Secondary joints are offset wherever they cross primary joints, and tertiary joints are offset when crossing both primary and secondary joints. This means that three fundamentally different joint characters are modelled. The use of other intersection angles will add to the variety.

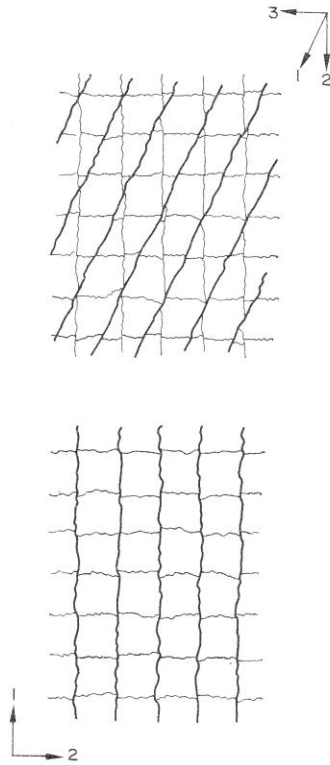


FIG. 5. Sections illustrating the offsets of secondary and tertiary joints.

The genesis and description of rock joints is a controversial topic among structural geologists. However, it can be said with certainty that joints can develop at practically all ages during a rock's history. Denudation and isostatic uplift can cause gradual but dramatic changes in the external stress environment, and in combination with the stored strain energy of the rocks, the development of both tension and shear joints can be explained (PRICE [13]). It is certainly difficult to envisage that all joint sets are the direct result of tensile stresses acting perpendicularly to the joint planes, since it would be necessary to postulate a complex and changing stress system to account for each set of joints. The feature which is difficult to explain is the lack of displacement across shear joints. The plume structures which occur on many of such joints have delicate relief, and any significant differential movement along the joints would completely obliterate the markings.

It would seem that the jointed model can provide a very realistic simulation of the following structural system. The primary continuous joints, which are not offset when intersected by subsequent joints, can be regarded as a set of master shear joints which, because of continuity exhibit the lowest shear strength. The secondary and tertiary joints are clearly tension joints and their offset, stepped nature means that their shear strength is considerably higher. It would appear that a tension fracture cannot propagate perfectly (without offset) across a pre-existing fracture, unless the latter is tightly closed as a result of a favourable stress system.

Before presenting detailed results of the strength-deformation properties of these model tension joints it is wise to record the areas of doubt surrounding one or two aspects of the scaling. The controversial results which are to be presented can then be viewed in a more objective and informed manner.

1. The model roughness is considerable and should be scaled up and interpreted accordingly. Large-scale exposures of joints having lower degrees of roughness will have reduced strength and deformation characteristics compared to the model prediction.
2. The model joints are completely free of soft infilling material, unlike many joints encountered in field excavations. Likewise the joint walls are fresh fractures and are therefore unaltered by weathering.

#### DIRECT SHEAR TESTS OF MODEL TENSION JOINTS

A standard soil mechanics range,  $6 \times 6$ -cm shear box was used for all the shear tests. However, two small modifications were required for testing model joints. Firstly, the two split halves of the shear box were separated by a  $\frac{1}{8}$  in. strip of P.T.F.E. (Teflon) low-friction compound. Single, primary tension joints were generated in rectangular blocks of the model material, such that the mean horizontal joint plane lay within the gap between the separated halves of the box. Secondly, a light duralumin platen, loading yoke, four wires and hanger were substituted for the conventional normal load device. The latter was heavy enough to cause compressive failure of the weakest model material, even without additional weights. In view of the low strength of the model joints, the proving ring used for applying and measuring the shear force can be considered as an extremely stiff system. It was possible to follow all the post-peak behaviour accurately.

TABLE 2. MODEL-PROTOTYPE SHEAR TEST PARAMETERS

Parameter	Model	Prototype	Scale
Dimension	$2.32 \times 1.00$ (in.)	$96 \times 42$ (ft)	$\lambda = 500$
Total displacement	0.18(in.)	7.5(ft)	$\lambda = 500$
Rate of shear	0.046 (in/min)	1.03 (in/min)	$\lambda^2 = 22.5$
Normal stress	(lbf/in <sup>2</sup> )	(lbf/in <sup>2</sup> )	
1	0.044	29.3	} $\psi = 666$
2	0.168	112	
3	0.286	191	
4	0.477	318	
5	0.668	445	
6	0.954	635	
7	1.620	1080	
8	2.383	1589	

Figure 6 illustrates sixteen pairs (upper and lower mating halves) of rectangular shear specimens which had previously been sheared at a variety of normal stresses. The lowest stress was applied to specimens P.C.1 and P.C.2, and the highest to specimens P.C.15 and P.C.16. The ultimate shear displacement was 0.18 in. which represented 7.7 per cent of the total length of each specimen. The previous table compares the model and prototype test parameters, for an assumed geometric scale ( $\lambda$ ) of 1:500.

The lowest normal stress was applied by nothing more than the weight of the upper half of the block lying above the tension joint. This represented model and prototype 'overburdens' of 0.63 in. and 26 ft respectively. As a result of this low stress virtually no shear damage could be detected. (See specimens P.C.1 and P.C.2, Fig. 6.)

*Strength envelopes of three model tension joints*

The inset to Fig. 7 illustrates three types of tension joint which can be generated on the large guillotine. It was of interest to see if there was any difference in shear strength between a single primary joint, and one with cross joints generated after the primary joint. (These have been termed: primary cross-jointed P.C.J.) A greater strength was obviously to be expected of the purely secondary joint, with its characteristic offsets.

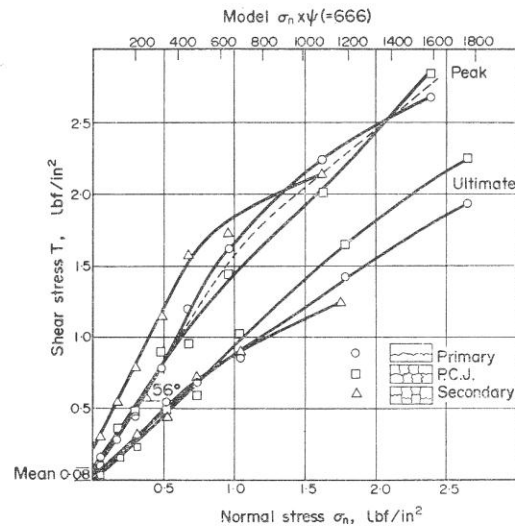


FIG. 7. The shear-strength envelopes of three tension-joint characters in model material C3.

Each point plotted in Fig. 7 is the mean of two tests conducted at the same normal stress. The angle of friction of 56° and the cohesion intercept of 0.08 lbf/in<sup>2</sup> are tentative, linear approximations to the lower part of the peak-strength curve for the continuous primary joints. It has been convincingly demonstrated that even for joints as rough as those tested, no true cohesion exists, the peak-strength envelope merely becoming tangential to the ordinate at the origin (BARTON [14]). However, secondary joints with perpendicular cross joints obviously will have cohesion, and a value of approximately 0.2 lbf/in<sup>2</sup> is indicated.

The ultimate curves demonstrate that a shear 'strain' of 7.7 per cent (0.18 in. displacement) is insufficient to reach the true residual strengths. In fact a series of residual tests on

flat surfaces of the same model material gave a mean friction angle of  $28\frac{1}{2}^\circ$ . In practice it is difficult to see how a rough tension joint can have its shear strength reduced to around  $30^\circ$  by the mechanism of increased shear displacement, unless the normal stress is extremely high. Weathering and alteration of the joint walls might be required if true residual strength is to be reached under low levels of normal stress.

Figure 8 illustrates the effect of normal stress on the relative drop from peak to ultimate strength. The interlock effect in the secondary joint surfaces is clearly shown by the large ratio (16.6:1) of peak to ultimate strength at the lowest normal stress. The curves appear to become asymptotic to a ratio of 1:1 as the normal stress increases. This might be expected at extremely high stresses, when the presence of joints has limited effect on the strength and deformation.

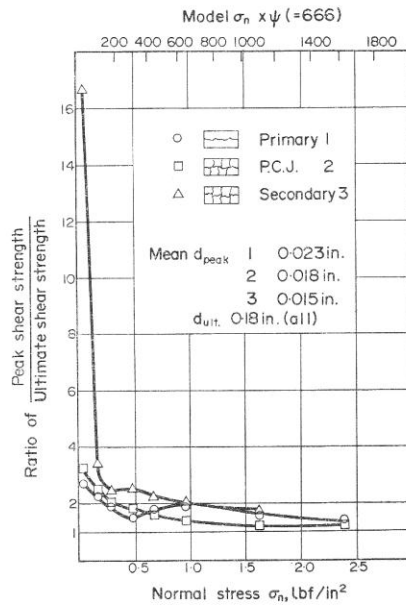


FIG. 8. The ratio of peak to ultimate strength as a function of normal stress for three tension joints in model material C3.

#### Shear force-displacement relationships

Figures 9 and 10 illustrate the magnitudes of the normal and tangential displacements which accompany shear failure. It will be noted that in each case the predicted prototype displacement is given on a separate scale at the top of each figure. The curve numbering (1-8) signifies the normal stress applied in each case, which was listed in Table 2.

It is customary to expect peak tangential (horizontal) displacements of less than  $\frac{1}{2}$  in. even for *in situ* shear tests. (See comprehensive review article by GOODMAN [15].) It will therefore be of some surprise to find predicted peak displacements for a  $96 \times 42$  ft prototype joint, ranging from about 5 to 15 in. However, when it is realized that the hypothetical joint dimension is almost an order of magnitude greater than the largest *in situ* tests performed, the large displacements become more realistic. Their relevance to *in situ* conditions

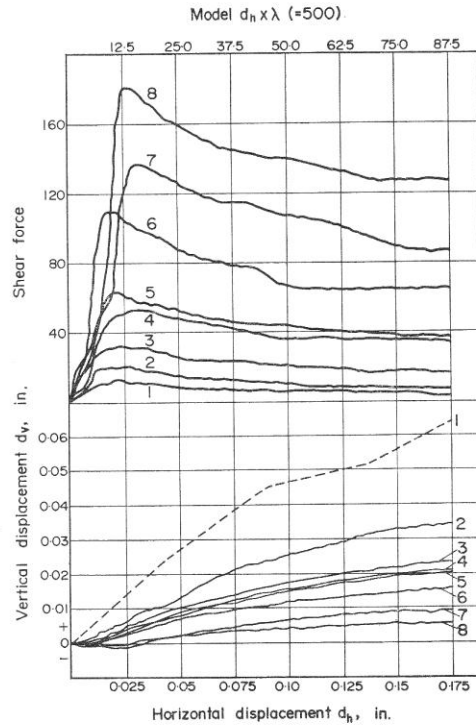


FIG. 9. Shear force-displacement and dilation characteristics for primary tension joints in model material C3.

will depend primarily on the joint roughness 'waveform' found in the field. A roughness of long wavelength which might be typical of a tension joint in granite can be expected to induce much larger displacements before failure (peak) than a more planar shear joint. (A series of shear tests using model materials of different strengths to simulate test dimensions ranging from  $7\frac{1}{2}$  to 96 ft, revealed that the peak strength for rough joints was reached after a displacement of approximately 1 per cent of the test length, throughout this range of dimensions—BARTON [14].)

The normal or vertical displacement accompanying shear of rough joints is of course considerable. It will be noted from Figs 9 and 10 that most of the total dilation takes place after peak strength is reached. In fact no total dilation is necessary for peak shear strength to be reached under the two highest normal stresses. The dilatency effect is still operating but some contraction occurs after a small horizontal displacement. This can be interpreted as increased interlocking of the mating asperities. At prototype scale the peak shear strength is mobilized after a dilation of less than  $2\frac{1}{2}$  in. for all but the two lowest normal stresses. Note that the maximum angle of dilation ( $d_v/d_h$ ) occurs approximately at the instant when peak strength is mobilized. This observation forms the basis of a peak-strength criterion for rock joints (BARTON [14]).

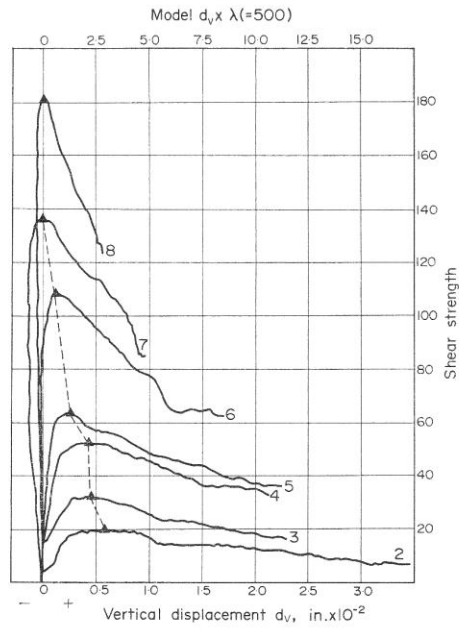


FIG. 10. The relationship between shear strength and normal displacement for primary tension joints in model material C3.

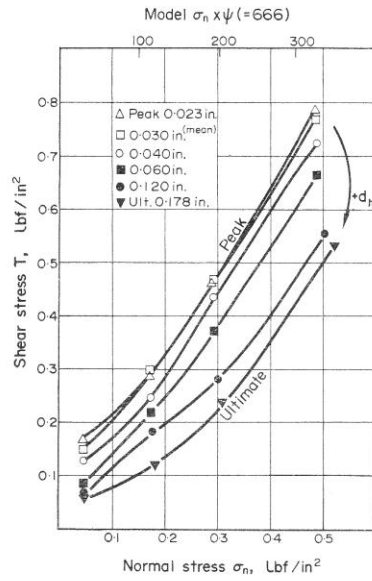


FIG. 11. The post-peak shear-strength behaviour of primary tension joints in model material C3, at low normal stresses.

*Stress dependence of pre-peak and post-peak displacements*

It is probably true to say that post-peak shear displacements are, by their very nature, of more interest to the mining industry, than to civil engineers involved in surface excavations. It must be seldom that post-peak behaviour can be tolerated in engineering structures, whereas large shear displacements and tension cracks are accepted as partners to high ore-waste ratios in open cast mines.

KRSMANOVIC [16] presented shear-strength envelopes for rock joints plotted to a common displacement, to demonstrate the post-peak shear strength remaining after a given total displacement. This is clearly of interest and the same procedure has been adopted here in Fig. 11 for the model tension joints. The inverted curvature of the envelopes is also demonstrated by some of Krsmanovic's results, although it is unusual for the peak envelope.

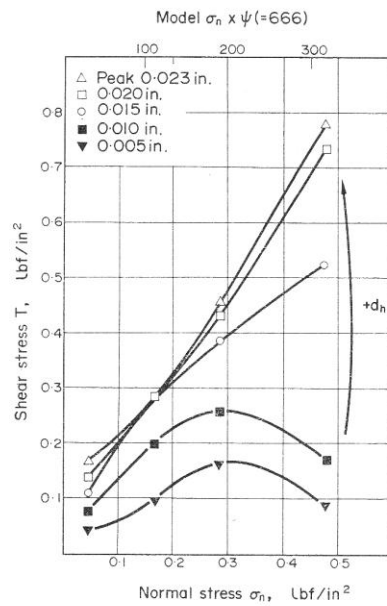


FIG. 12. The pre-peak shear-strength behaviour of primary tension joints in model material C3, at low normal stresses.

From an engineering point of view the pre-peak behaviour shown in Fig. 12 is of more immediate interest. It demonstrates the simple yet unexpected result that a joint has no strength until displaced slightly. This lends support to the rock bolt adage: "help the rock to help itself". The lowest curve represents the shear strength mobilized for a common displacement of  $2\frac{1}{2}$  in. at prototype scale. This displacement mobilizes only about 10 per cent of the peak shear strength when the normal stress is over 300 lbf/in<sup>2</sup>, but over 30 per cent at lower stresses.

**STIFFNESS OF MODEL JOINTS**

The 'stiffness' of a rock joint is a term of relatively recent origin and is used to describe the overall stress-deformation characteristic; both in the normal and tangential sense. It is

becoming widely used in finite-element models of jointed rock. In its simplest form essentially two components are considered (GOODMAN *et al.* [1]). The normal stiffness is defined as the normal stress per unit closure of the joint, and the shear stiffness is the mean gradient of the shear stress–shear displacement curve, taken up to the point of peak strength. Both have units of  $\text{lb}/\text{in}^2$  per in. If a ‘failure analysis’ is being performed a residual shear stiffness may also be used.

The use of these three deformation components in finite-element analyses has preceded the more recent attempts to model strain softening characteristics more fully, such as those reported by ZIENKIEWICZ *et al.* [3].

#### Normal stiffness of model tension joints

Numerous *in situ* plate-jacking tests have indicated that the  $E$ -modulus of a rock mass may be as much as an order of magnitude less than the modulus measured from tests on unjointed laboratory specimens. This is because the normal stiffness of joints is generally considerably lower than that of the intact rock separating the joints, depending of course upon the joint spacing. It is of interest to see how the jointed model fits this general observation.

Normal loading and unloading tests were carried out in the same shear box that was used for the shear tests. However, only the normal loading system was used. The joint dimensions were also identical to those tested in shear and represented prototype joint surfaces of  $96 \times 42$  ft.

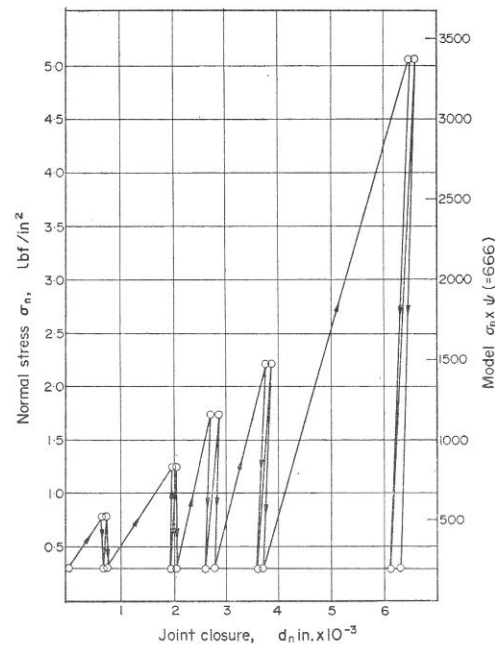


FIG. 13. The effect of normal stress cycles on the closure of primary tension joints in model material C3.

It can be seen from Fig. 13 that a datum normal stress of  $0.30 \text{ lbf/in}^2$  was applied throughout. This was unavoidable since the vertical displacement and loading systems had to be applied via a light platen and loading yoke. These could not be removed between the normal load cycles without disturbing the joints. The results shown are the mean of tests on three model joints generated in model material C3. Similar results were obtained for secondary joints, and for primary joints in a weaker model material.

The first cycle of loading at each stress level produced a large and more or less irrecoverable closure of the joints. The load was applied for several minutes to preconsolidate the joints, though in fact this proved unnecessary since the final deformation was immediately registered. The load was then reduced to the datum and carefully reapplied to produce an approximate stiffness line. The joint closures presented in Fig. 13 have been corrected for the elastic displacements predicted for the solid material above and below the joint in the loading box. It should be noted that the maximum normal stress applied ( $5.07 \text{ lbf/in}^2$ ) is approximately one-quarter of the unconfined compression strength of the intact material.

Table 3 summarizes the model normal stiffness results and gives the prototype equivalents predicted from geometric and stress scales of 1:500 and 1:666 respectively. The conversion factor between model and prototype is the ratio  $(\psi/\lambda)$ .

TABLE 3. MODEL-PROTOTYPE NORMAL STIFFNESS AS A FUNCTION OF CONSOLIDATION STRESS

Consolidation stress (lbf/in <sup>2</sup> )		Normal stiffness $K_n$ (lbf/in <sup>2</sup> /in)	
Model	Prototype	Model	Prototype
0.774	516	$1.54 \times 10^4$	$2.04 \times 10^4$
1.249	832	$1.09 \times 10^4$	$1.45 \times 10^4$
1.726	1150	$0.53 \times 10^4$	$0.70 \times 10^4$
2.201	1468	$0.76 \times 10^4$	$1.01 \times 10^4$
5.067	3377	$0.93 \times 10^4$	$1.23 \times 10^4$

It can be seen that the normal stiffness under intermediate stresses is smaller than that of both lower and higher stress levels. This unexpected trend is shown in Fig. 14 (a). A mechanism of 'normal failure' seems to be required to explain it.

The first cycle of loading at each stress level consolidates the joints causing mostly irrecoverable closure appropriate to the stress level applied. This constitutes a loading history, thereby colouring subsequent behaviour just as would be expected in the field. The anomalous result for intermediate stress levels is perhaps due to the interaction of three modes of deformation.

1. Small elastic displacements at low stress causing stiff behaviour.
2. Loosening and slight rolling of particles on the asperity slopes at intermediate stress.
3. Large increases in true contact area at high stress causing restiffening.

#### *Comparison with normal stiffness of rock masses*

A large number of plate-jacking tests are reported in rock mechanics literature. These are most commonly performed at dam sites in an attempt to obtain a deformation modulus for the rock mass, for comparison with the  $E$ -modulus of the concrete dam. Due to the complexity of the jointing and the uncertain nature of the normal stress distribution, it is almost

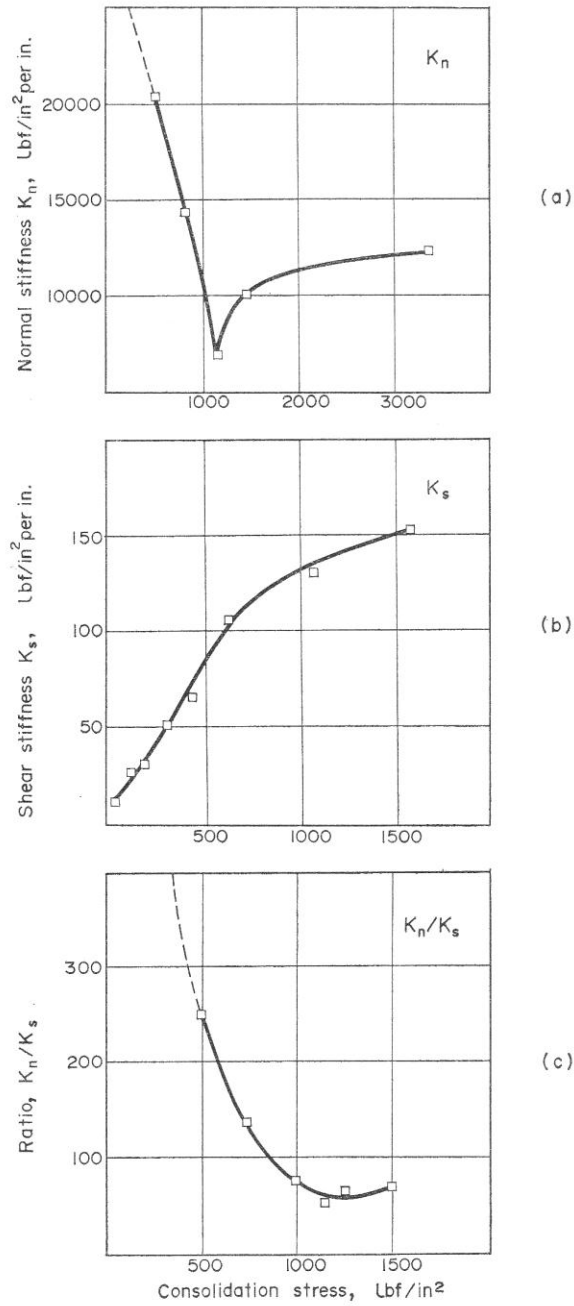


FIG. 14. The joint stiffness relationship for prototype joints as a function of the preconsolidation stress level.

impossible to estimate the deformation performance of one joint set. Consequently although much data exists concerning the ratio ( $E_{mass}/E_{intact}$ ) the actual normal stiffness value is missing.

However, attention has recently been focused on the possible influence of the state of stress on the joint water flow in rock masses. Several authors have considered this problem and it is to be hoped that some much needed information on joint normal stiffness will ensue, both for this problem and the more general finite element simulation of rock masses.

Some useful data on plate-bearing tests that were performed during a comprehensive series of *in situ* tests at a French dam site have been given by LOUIS [17]. The dam was constructed on more or less horizontally bedded limestone with conveniently regular systems of discontinuities. Many of these were found to contain thin seams of sandy marl. A comparison of the deformation performance of the joints with laboratory tests on the intact limestone showed the following approximate results:

$$\begin{aligned} \text{Rock mass } E_m &= 710,000 \text{ lbf/in}^2 \\ \text{Intact rock } E_i &= 7,100,000 \text{ lbf/in}^2 \end{aligned}$$

The *in situ* loading tests were performed perpendicular to the bedding joints, which had a mean spacing of approximately 24 in. Knowing the spacing it is possible to estimate the normal stiffness of individual bedding joints from the following relation:

$$E_m/E_i = \left[ \frac{K_n \cdot L}{K_n \cdot L + E_i} \right] \tag{1}$$

where

- $E_m$  is the deformation modulus of the rock mass
- $E_i$  is the deformation modulus of the intact rock
- $K_n$  is the normal stiffness of individual joints
- $L$  is the mean joint spacing.

Substitution of the values given by Louis in the above equation gives the following estimate of normal stiffness:

$$K_n = 3.34 \times 10^4 \text{ lbf/in}^2/\text{in.}$$

The dimension of intact limestone with the same normal stiffness as one average joint is equal to the ratio ( $E_i/K_n$ ) = 17.7 ft.

These calculations will now be applied to the model joints for comparison. The model and prototype values of ( $E_i$ ) are  $1.07 \times 10^4$  and  $7.13 \times 10^6$  lbf/in<sup>2</sup> respectively. (The similarity with the  $E$ -modulus of limestone is entirely fortuitous.)

TABLE 4. DIMENSION OF INTACT MATERIAL WITH EQUAL STIFFNESS TO ONE MODEL JOINT

Model		Prototype		
Normal stress (lbf/in <sup>2</sup> )	$E_i/K_n$ (in.)	Normal stress (lbf/in <sup>2</sup> )	$E_i/K_n$ (in.)	$E_i/K_n$ (ft)
0.774	0.70	516	350	29
1.249	0.99	832	492	41
1.726	2.02	1150	1013	84
2.201	1.41	1468	706	59
5.067	1.15	3377	578	48

It is not known at what stress the *in situ* tests were performed. However, it would seem very unlikely to have been as high as even the lowest prototype stress (516 lbf/in<sup>2</sup>). In view of the trend shown in Fig. 14 (a), the model would appear to produce a prototype stiffness quite close to that of the limestone, when interpreted at a lower and more relevant normal stress.

The ratio of ( $E_m/E_t$ ) can also be calculated for the jointed model by doing the previous calculations in reverse. Since this ratio is a dimensionless number both model, prototype and reality should all have the same ratios for correct scaling to be achieved. For simplicity only one set of parallel joints will be considered. Equation (1) gives the following ratios of ( $E_m/E_t$ ) based on a model-prototype joint spacing of  $\frac{1}{2}$  in/20.8 ft.

$$1/2 \cdot 4, \quad 1/3 \cdot 0, \quad 1/5 \cdot 0, \quad 1/3 \cdot 8, \quad 1/3 \cdot 3.$$

These values are for the five normal stresses (preconsolidation stresses) listed in Table 4.

The results of *in situ* measurements carried out at several dam sites in the U.S.A. were the subject of a recent study by COON and MERRITT [18]. The majority of tests on gneisses, limestones and sandstones gave values of ( $E_m/E_t$ ) within the range 1/10–1/2.5. The model joint spacing is therefore seen to give quite representative values, and by decreasing it to  $\frac{1}{4}$  in. or increasing it to 1 in. the complete range can be obtained.

The anomalous nature of the model-prototype results shown in Fig. 14 (a) has already been referred to. For some reason the normal stiffness appears to reduce to some minimum value with increasing stress, and consequently to rise as the joint becomes more closed at high stress. Coon and Merritt show a load-deformation curve obtained from a plate-jacking test in which the apparent stiffness is shown to reduce with increasing normal stress over the range 500–1000 lbf/in<sup>2</sup>. They concede that the modulus may increase or decrease with increasing stress levels. However, it seems certain that any joint containing a thin layer of clay would demonstrate a stiffening behaviour with increasing levels of stress. Perhaps this intuitive observation cannot be applied to predict the stiffness behaviour of unweathered joints. Obviously there is much to be learnt about the mechanism of joint closure.

#### *Shear stiffness of model tension joints*

The shear stiffness of a joint was defined as the ratio of the peak shear stress to the shear displacement at this peak. It may have been noticed from Fig. 9 that there was no marked increase in peak shear displacement with increasing levels of normal stress. For this reason one would expect considerable variation in shear stiffness for different levels of normal stress.

Table 5 shows the mean shear stiffness for the three types of tension joint generated in material C3 (see inset to Fig. 8). Model stiffness is shown scaled up to the prototype stiffness in the right-hand columns.

The mean trend demonstrated by the primary and primary cross-jointed surfaces is shown in Fig. 14 (b) at prototype scale. As plotted there is a close relationship between the shape of this curve and the peak shear-strength envelope (Fig. 7). This is a direct result of the limited dependence of peak displacement on the level of normal stress.

Figure 14 (c) shows the mean ratio of normal to shear stiffness as a function of consolidation stress. It is unfortunately impossible to compare the two stiffnesses below a prototype preconsolidation stress of 500 lbf/in<sup>2</sup>. However, it would appear from a tentative extrapolation that the ratio ( $K_n/K_s$ ) might rise to between 500 and 1000 at stress levels appropriate to near-surface excavations. It therefore seems unquestionable that for unweathered joints in rock the stiffness in shear is considerably lower than that in the normal direction. A

TABLE 5. SHEAR STIFFNESS OF MODEL AND PROTOTYPE JOINTS

$\sigma_n$ lbf/in <sup>2</sup>	Model			$\sigma_n$ lbf/in <sup>2</sup>	Prototype		
	$K_s$ lbf/in <sup>2</sup> /in Primary	P.C.J.	Secondary		$K_s$ lbf/in <sup>2</sup> /in Primary	P.C.J.	Secondary
0.044	7.4	12.0	43.0	29.3	9.8	15.9	57.1
0.168	24.2	17.8	49.0	112	32.2	23.7	65.4
0.286	18.2	30.0	43.3	191	24.2	40.0	57.8
0.477	31.0	46.5	63.7	318	41.3	62.1	84.7
0.668	49.3	51.0	78.8	445	65.8	68.0	105
0.954	84.0	77.5	123	635	112	103	164
1.620	102	96.2	112	1080	135	128	149
2.383	100	130	—	1589	133	172	—

N.B. No specimens of secondary joints were available for tests at the highest normal stress due to damage while handling them.

difference of two to three orders of magnitude appears a reasonable estimate for rough joints. These differences might be reversed by planar clay-filled joints.

#### Comparison with shear stiffness of rock mass

A cursory glance at the results of direct shear tests on rock joints leads one to believe that the model stiffnesses just presented are unrealistically low. As an example; the tests conducted by Pentz on natural joints in porphyry (referred to by GOODMAN *et al.* [1], and GOODMAN [15]) gave the following typical results:

Normal stress	= 895 lbf/in <sup>2</sup>
Peak shear stress	= 881 lbf/in <sup>2</sup>
Displacement at peak	= 0.26 in.

These figures imply a shear stiffness of 3450 lbf/in<sup>2</sup>/in for a joint approximately 9 in. square in area. By comparison, the model joints predict a shear stiffness of 125 lbf/in<sup>2</sup>/in for a 96 × 42 ft prototype joint at the same normal stress. This anomaly is not poor scaling but a simple demonstration of an important scale effect which does not appear to have been recognized.

A series of model shear tests have been described elsewhere (BARTON [6, 14]) in which an attempt was made to investigate whether a strength-size effect existed for joints. Model materials of widely different strengths ranging from approximately 10 to 120 lbf/in<sup>2</sup> in unconfined compression were used in the investigation. Tension joints were generated through the same size of block in each case, to produce joints of dimensions 2.3 × 1.0 in. as described earlier. However, since the joints were generated in different strengths of material, a simple dimensionless relationship could be used to convert the model tests to prototype joints having the same compressive strength but different test dimensions. The following table describes the properties of the four materials which were all manufactured from the same components: red lead-sand/ballotini-plaster-water. Different quantities of the cementing components were used to obtain the different strengths.

TABLE 6. MODEL-PROTOTYPE SCALING OF FOUR MATERIALS

Model material	$\sigma_c$ (lbf/in <sup>2</sup> )	$\rho$ (lbf/ft <sup>3</sup> )	$\lambda$	$\psi$	Prototype size (ft)	Prototype $\sigma_c$ (lbf/in <sup>2</sup> )
C2	10.2	120.7	500	666	96.0 × 42.0	} 6800 (lbf/in <sup>2</sup> )
C4	56.2	120.8	91	121	17.5 × 7.5	
C9	88.8	117.4	56	77	10.7 × 4.7	
C25	119.0	108.7	38.6	57	7.4 × 3.2	

Here

$\sigma_c$  is the unconfined compressive strength

$\rho$  is the density

$\lambda$  is the geometric scale

$\psi$  is the stress scale.

Each of the four models were tested at a different range of normal stress such that when these were converted to prototype stresses, the range for all four was the same and approximately 10–1600 lbf/in<sup>2</sup>. The results of the strength–size investigation in fact proved to be negative; no scale effect was found.

The feature which did not prove negative was the discovery of a displacement–size effect, which has an important bearing on the present stiffness investigation. The peak shear displacements for the four sizes of prototype joint surfaces were as follows:

TABLE 7

Size (ft)	Peak shear displacements (in.)
96.0 × 42.0	3.35–11.61
17.5 × 7.5	0.54–2.37
10.7 × 4.7	0.35–0.91
7.4 × 3.2	0.34–1.05

As a result of the negligible strength–size effect, large differences in shear stiffness are predicted for the four test dimensions. These results are plotted in Fig. 15, together with relevant stiffness data for tests on rock joints that were mostly obtained from GOODMAN's comprehensive review article [15]. Each model–prototype value is the mean of two shear tests at the same normal stress.

The test dimensions  $L$  (in.) was the square root of the test area reported by Goodman. In other words a square test area was assumed unless more specific data was available, as with the model joints, The stiffness data for the laboratory tests was obtained from reported tests on clean unfilled rock joints where possible. However, an unfortunate but inevitable feature of joint shear testing is that generally only difficult zones are tested, such as shear zones, clay-filled joints, planes of schistosity and so on. As a result it is difficult to collect a large body of data relevant specifically to clean unfilled joints, The data presented in Fig. 15 can be identified from Table 8. All but two of the sources were obtained from GOODMAN [15].

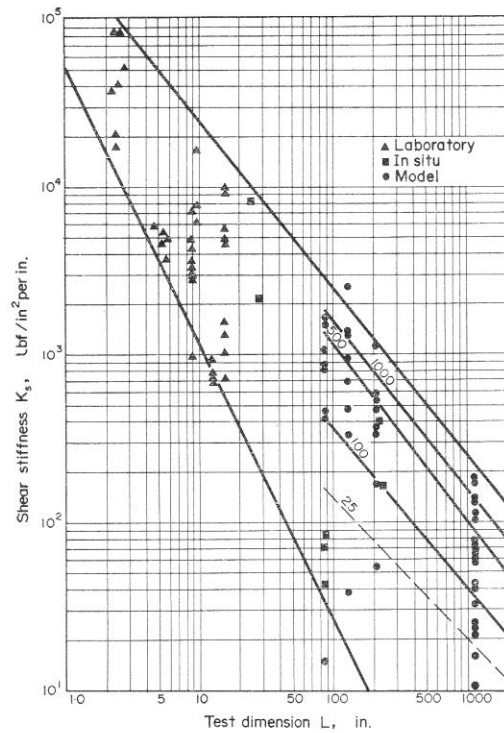


FIG. 15. Joint shear stiffness as a function of test dimensions and preconsolidation stress.

Four lines are drawn in Fig. 15 which span the model-prototype test results. These are marked 25, 100, 500 and 1000 and they are approximate envelopes for equal normal stress with units of  $\text{lbf/in}^2$ . Because of the scatter of results it was not feasible to extrapolate these lines into the laboratory test range. However, some of the large *in situ* test results do lie in the correct zone (Kujundzic, 88 in.), while others clearly do not. Two additional features are worthy of mention:

1. Krsmanovic's tests on rough and smooth unfilled fractures (15.8 in.) show values of shear stiffness which, with one exception, separate clearly into two groups. The mean stiffness for the rough joints is approximately five times as high as for the smooth.
2. The large number of model-prototype results plotted along the test dimension 1150 in. ( $96 \times 42$  ft) are the combined results for primary joints in materials C2 and C3 which had prototype unconfined compression strengths of 6800 and 13,400  $\text{lbf/in}^2$  respectively. The range of stiffness values are much the same for each. This is because the shear strength of C2 is slightly lower than that of C3, and at the same time, the peak displacements for the weaker material are also a little lower.

#### *Optimum test dimension for stiffness data*

An all-important question now arises. What size of test should be performed to obtain

TABLE 8. TEST DATA FOR SHEAR TESTS ON ROCK JOINTS

Source	Description of joints	Test dimensions (in.)	Normal stress (lbf/in <sup>2</sup> )
Coyne and Bellier	Limestone: dry marly joints Thickness of seams: 0.020-0.080 in.	2.2-2.7	71-213
De Freitas	Granite: rough dry joint from breaking beam	4.7-5.7	170-206
Pentz	Porphyry: dry natural joint surfaces	8.8 (approx.)	469-1450
Coyne and Bellier	Limestone: compact (oolitic) Limestone: stylonite (oolitic)	9.4 9.4	71 71
GIUSEPPE [20]	Phyllitic schist: foliation planes	12 (approx.)	28.4-213
Krsmanovic	Limestone: rough unfilled fractures Limestone: smooth unfilled fractures	15.8 15.8	220-579 128-340
Drozd	Greywacke: closed clean bedding Amphibolite: schistosity plane	23.8 23.8	62.5 17.7
Kujundzic	Closely jointed shale zone in limestone	88	2.8-3.0
Ruiz and Camargo	Unbonded contact between basalt and sandstone	218	18.2
RUIZ <i>et al.</i> [19]	Contact between compact basalt and breccia	233	24

stiffness data for a given size of field problem? Even with the benefit of the data displayed in Fig. 15 the decision is obviously fraught with uncertainty. It must be fair to say that the testing of a large area *in situ* will always give a more reliable result since, with careful control, the *in situ* conditions can be most easily maintained. This will be particularly true of joints containing soft infilling. However, in view of the expense of large numbers of *in situ* tests, there may be good reason to rely on the results of larger numbers of carefully sampled laboratory tests (6-12 in.), if the joints appear tightly closed and not unduly altered by weathering. The results obtained for shear stiffness will be strictly relevant to the test dimension, no larger or smaller, unless the joint exposures in the field display singular planarity like cleavage or foliation surfaces. However, if there appear to be several amplitudes (and wavelengths) of roughness depending upon the area of joint surveyed, then the guide lines exhibited by Fig. 15 may be very useful.

It will be noticed that the four equal stress lines for the model-prototype data are more or less parallel with the upper envelope. (The lower envelope is not similarly inclined, because of the discrepancy between the very low normal stress applied in some of the *in situ* tests, and the much higher stresses used in many of the laboratory tests.) The revealing feature of these equal stress lines is that they suggest an inverse proportionality between test dimension and shear stiffness. In other words for a given normal stress, a shear stiffness of 10,000 lbf/in<sup>2</sup>/in obtained from a 10-in. long laboratory specimen, would need to be reduced to 100 lbf/in<sup>2</sup>/in if a dam abutment was loading a 1000-in. length of joint in the field problem.

The normal stiffness probably presents less critical problems of measurement. According to the limited results presented earlier, the normal stiffness of one joint ranges from approximately the same order of magnitude to one order of magnitude less than the elastic normal stiffness of the intact rock between the joints. For example, a rock having an intact ( $E$ ) modulus of  $7 \times 10^6$  lbf/in<sup>2</sup> will have normal block stiffnesses—ranging from 350,000 to 35,000 lbf/in<sup>2</sup>/in for joint spacings of 20 and 200 in. respectively. The lower value of stiffness corresponds to the normal stiffness obtained from the *in situ* test in limestone, and the model-prototype values when projected to an engineering range of stresses. Both normal stiffness components can therefore be considered as much less critical to the total deformation than the shear stiffness, and small errors in the measurement of either of them will be negligible compared to ignorance of the size effect for shear stiffness. (These generalizations cannot be applied to joints containing a significant thickness of soft infilling material.)

It has been noted by SNOW [21] that the normal deformation modulus of fractured rocks depends in part upon the size of sample. Plate-jacking tests give smaller moduli than laboratory tests, and chamber-pressure tests smaller still. It appears that the joint water-boundary conditions will also have some effect. The modulus will be lower if joint water pressure can be dissipated at the water table, than if fully confined.

While these effects are irrefutable, they would appear to be purely a function of sampling size; larger tests reach more major joints and vice versa. In view of the extreme importance of shear and normal stiffness data to numerical and physical modelling, what is most desirable is to conduct cyclic normal stiffness tests on specific single-jointed samples before the latter are tested in shear at the same normal stress. (It appears to be very important not to preconsolidate a joint, and then shear it at a lower normal stress. A significant artificial increase in shear strength, and hence shear stiffness, may be registered—see BARTON [6].) If the above procedures are adopted and the joint sampling is representative, any possible normal stiffness-size effect will be minimized.

#### *Requirements for numerical simulation of rock-joint deformation*

It has been shown that for relatively wide joint spacing the normal stiffness of the joints may be roughly the same order of magnitude as the elastic normal stiffness of the intervening intact rock. This comparison will now be extended to shear stiffness.

The elastic shear modulus ( $\mu$ ) is related to the normal modulus ( $E$ ) as follows:

$$\mu = \frac{E}{2(1 + \nu)} \quad (2)$$

where  $\nu$  is Poisson's ratio of the rock. A typical value for the latter is 0.2, and taking the same  $E$ -modulus of  $7 \times 10^6$  lbf/in<sup>2</sup> the shear modulus is found to be approximately  $3 \times 10^6$  lbf/in<sup>2</sup>. The elastic shear stiffness of the intact rock between joints spaced at 20 and 200 in. will therefore be 150,000 and 15,000 lbf/in<sup>2</sup>/in respectively. Even the lowest of these two values can be as much as three orders of magnitude stiffer in shear than one 100-ft long joint, according to the stiffness-size effect illustrated in Fig. 15.

It would therefore appear conclusive that a numerical analysis of jointed rock that incorporated only the elastic stiffnesses of the intact rock would give quite meaningless results unless it could be established that the jointing was sporadic and non-continuous, or that the *in situ* stresses were so high that existing joints remained tightly closed in spite of disturbance by excavation.

It has been shown by ST JOHN [4] and BARTON [6] that an even more inaccurate deformation picture is obtained if the stiffnesses of the joints are linearly superimposed on the elastic properties of the intact rock. Anisotropic elastic continuum analyses of rock-slope behaviour using the finite-element method produce grossly exaggerated 'elastic recovery' displacements which have no relevance to reality since such large deformations can only be non-elastic and irrecoverable. It seems unquestionable that shear deformation of joints is largely irrecoverable, even just up to the development of peak shear strength. The extreme 'softness' of joints in shear means that even slight inelasticity here will make the overall behaviour grossly inelastic in reality.

The present use of line-joint elements for two-dimensional studies (GOODMAN *et al.* [1], DUNCAN and GOODMAN [22] and ST JOHN [4]) and triangular or quadrilateral-shaped elements for three-dimensional studies (MAHTAB and GOODMAN [2] and ST JOHN [4]) has obviously improved numerical modelling considerably. However, certain problems seem to have been encountered which may or may not be solved by future improvements in computing methods.

1. The elastic stiffness characteristics of the joint elements should not differ from those of adjacent solid elements by large amounts or else danger of ill conditioning of the assembled elastic equations will exist. ZIENKIEWICZ *et al.* [3] have suggested that a ratio of 1:1000 should not in general be exceeded. Despite certain differences in approach it may be significant that extremely low values of  $E$ -modulus tend to be used in many numerical examples published in the literature. [1,2]. The fact that joint stresses are insensitive to reductions in  $E$ -modulus does not mean that the overall deformation behaviour is going to be unaffected by unrealistic assumptions.
2. There appears to be an ever-present problem of non-uniqueness of solution when new and untried problems are tackled. The only fool-proof solution would be the construction of sophisticated physical models as a check on the numerical solutions.
3. Finite-element modelling of post-peak behaviour of jointed rock is complicated by the fact that the co-ordinates defining line-joint elements should not become overlapped during the modelling of slip on the joints. In extreme cases this may limit the concentration of the element mesh, such as that chosen to closely define the behaviour around an excavation.
4. A fundamental requirement of the finite-element method is the conservation of energy demanded during computation. It is for this reason that anisotropic continuum analyses predict such an impossibly large 'elastic recovery' when simulating excavation in rock. In reality energy is dissipated in friction and asperity failure along the joints, and should therefore be 'dissipated' in the numerical analyses if they are to be realistic. This will be even more true for post-peak behaviour than pre-peak behaviour.

The 'finite difference' approach adopted by CUNDALL [5] appears to overcome most of these problems. Cundall has dispensed with the concept of stresses and strains and has developed a programme which deals with the forces and displacements existing within a system of discrete blocks. Multiple block models are loaded in any desired manner and the deformations and mass failure movements resulting from removal of critical blocks (excavation) are plotted by computer for given increments of time. The components of mass deformation illustrated include joint consolidation, simple shear, toppling and rotation all plotted at true scale. These progressive failure plots closely resemble the failures induced by excavation of slopes in conventional (smooth brick) physical models—see HOFMANN [23].

5. Due to limitations of computer storage and inadequate input data the normal displacement accompanying shear failure of a joint has not been modelled systematically. Individual joints with teeth have been studied (GOODMAN *et al.* [1], ST JOHN [4]), but the method is unfortunately too uneconomical on computer storage for application to realistic jointed rock masses.

The omission of dilation effects in numerical and most physical models of jointed rock is more serious than it may appear. The amount of dilation which occurs before peak strength is reached may be only a fraction of that occurring on the way to residual strength if the joint is undulating on a large scale (see Fig. 9). Yet this small pre-peak dilation is itself orders of magnitude larger than any normal stiffness effects.

When a set of parallel joints in rock are subjected to shearing stresses it is usually anticipated that failure will occur on all the joints that suffer shear stresses in excess of their peak shear strength at the existing levels of normal stress. However, in a situation with more or less fixed external boundaries (i.e. underground excavations) considerable increases in normal stress may accompany the dilation. This being the case major shear displacements will be inhibited and will only occur on a small number of joints, most likely only on one. (In soil mechanics terminology the rock mass would be described as 'denser than critical' and therefore dilates during shear instead of contracting as might loosely dumped rock fill.)

Joints which are probably exceptions to the 'dilation during shear' behaviour are:

- (a) smooth cleavage surfaces such as in slates
- (b) severely weathered, planar surfaces such as bedding joints
- (c) joints near an excavation opened and displaced by blast damage
- (d) clay-filled joints of significant thickness.

#### CONCLUSIONS

In view of all the present difficulties in numerical simulation of jointed rocks, a widespread move to realistic physical modelling might not be the retrograde step that it has often appeared. The biggest single difficulty in rock mechanics will probably always be the measurement and understanding of relevant input concerning joint characteristics. Numerical methods can never solve this problem and the relevance of numerical output is completely dependent on the relevance of the input assumptions. Realistic physical models can contribute something to an understanding of both input and output.

#### REFERENCES

1. GOODMAN R. E., TAYLOR R. L. and BREKKE T. L. A model for the mechanics of jointed rock. *Proc. Am. Soc. civ. Engrs* SM3 94, 637-659 (1968).
2. MAHTAB M. A. and GOODMAN R. E. Three-dimensional Finite Element Analysis of Jointed Rock Slopes, *Proceedings of the Second Congress of the International Society for Rock Mechanics*, Belgrade, Vol. 3, (1970).
3. ZIENKIEWICZ O. C., BEST B., DULLAGE C. and STAGG K. G. Analysis of Non-linear Problems in Rock Mechanics with Particular Reference to Jointed Rock Systems, *Proceedings of the Second Congress of the International Society for Rock Mechanics*, Belgrade, Vol. 3 (1970).
4. ST JOHN C. M. Ph.D. Thesis, University of London. To be published.
5. CUNDALL P. A. *The Measurement and Analysis of Accelerations in Rock Slopes*, Ph.D. Thesis, University of London (1971).
6. BARTON N. R. *A Model Study of the Behaviour of Steep Excavated Rock Slopes*, Ph.D. Thesis, University of London (1971).
7. STIMPSON B. Modelling materials for engineering rock mechanics. *Int. J. Rock Mech. Min. Sci.* 7, 77-121 (1970).
8. FUMAGALLI E. Model Simulation of Rock Mechanics Problems, in *Rock Mechanics in Engineering Practice*, Chap. 11, Wiley (1968).

9. LADANYI B. and ARCHAMBAULT G. Simulation of Shear Behaviour of a Jointed Rock Mass, *Proceedings of the Eleventh Symposium on Rock Mechanics*, Berkeley (1969).
10. KRSMANOVIC D., TUFO M. and LANGOF Z. Shear Strength of Rock Masses and Possibilities of its Reproduction on Models, *Proceedings of the First Congress of the International Society for Rock Mechanics*, Lisbon, pp. 537-542 (1966).
11. PATTON F. D. *Multiple Modes of Shear Failure in Rock and Related Materials*, Ph.D. Thesis, University of Illinois (1966).
12. BARTON N. R. A Low Strength Model Material for Simulation of the Mechanical Properties of Intact Rock in Rock Mechanics Models, *Proceedings of the Second Congress of the International Society for Rock Mechanics*, Belgrade, Vol. 2 (1970).
13. PRICE N. J. *Fault and Joint Development in Brittle and Semi-brittle Rock*, Pergamon Press, Oxford (1966).
14. BARTON N. R. A Relationship Between Joint Roughness and Joint Shear Strength, *Proceedings of the International Rock Mechanics Symposium: "Fissuration des roches"*, Nancy (1971).
15. GOODMAN R. E. The deformability of joints. Determination of the *in situ* modulus of deformation of rock. *Proc. Am. Soc. Test. Mater.* STP 477, 174-196 (1970).
16. KRSMANOVIC D. Initial and residual shear strength of hard rocks. *Géotechnique* 17, (2) 145-160 (1967).
17. LOUIS C. Private communication (1970).
18. COON R. F. and MERRITT A. H. Predicting the *in situ* modulus of deformation of rock. *Proc. Am. Soc. Test Mater.* STP 477, 154-173 (1970).
19. RUIZ M. D., CAMARGO F. P., MIDEA N. F. and NIEBLE C. M. Some Considerations Regarding the Shear Strength of Rock Masses, *Proceedings of the Rock Mechanics Symposium*, Madrid, pp. 159-169 (1968).
20. GIUSEPPE B. The Shear Strength of some Rocks by Laboratory Tests, *Proceedings of the Second Congress of the International Society for Rock Mechanics*, Belgrade, Vol. 2 (1970).
21. SNOW D. T. Fracture deformation and changes of permeability and storage upon changes of fluid pressure. *Colo. Sch. Mines Q.* 63 (1), 201-244 (1968).
22. DUNCAN J. M. and GOODMAN R. E. *Finite Element Analysis of Slopes in Jointed Rock*, Contract Report S.68.3 for Corps of Engineers, Mississippi (1968).
23. HOFMANN H. The Deformation Process of a Regularly Jointed Discontinuum During the Excavation of a Cut, *Proceedings of the Second Congress of the International Society for Rock Mechanics*, Belgrade, Vol. 3 (1970).